ChemPubSoc Europe

DOI: 10.1002/chem.201801051

CHEMISTRY A European Journal Full Paper

Photochemistry

Photoregulating Antifouling and Bioadhesion Functional Coating Surface Based on Spiropyran

Leixiao Yu,[a] Christoph Schlaich,[a] Yong Hou,[a] Jianguang Zhang,[a] Paul-Ludwig Michael Noeske,[b] and Rainer Haag*[a]

Abstract: Dynamic regulation of the interactions between specific molecules on functional surfaces and biomolecules, for example, proteins or cells, is critical for biosensor and biomedical devices. Herein, we present a spiropyran (SP)-based light-responsive surface coating, hPG (hyperbranched polyglycerol)-SP, to control the adsorption of proteins and adhesion of cells. In the normal state, the SP groups on the coating surface were in hydrophobic ring-closed form, which promotes the nonspecific protein adsorption and cell adhesion. Under UV irradiation, the grafted SP groups were dynamically isomerized into hydrophilic/zwitterionic merocyanine. Both hydrophilicity and zwitterions support the formation of a hydrated layer and hence the resulting hPG-MC coatings highly resist protein adsorption and cell adhesion. Moreover, the presented hPG also provided a robust bioinert background to suppress the nonspecific protein adsorption and cells adhesion. Therefore, this functionalized coating exhibited a good photoregulated antifouling behavior. Moreover, the detachment of adsorbed proteins and adhered cells from the coating surface was also realized.

Introduction

Surface biofouling, which is mainly caused by spontaneous nonspecific protein adsorption, is a ubiquitous and serious problem that may stimulate deleterious biological processes orchestrated by the immune and coagulation systems. It has greatly limited the application of biomaterials in medical implants, surgical equipment, biosensors, etc.[1] The nonspecific protein adsorption on materials is often associated with surface hydrophobicity.[2] Proteins undergo a conformational change to associate their hydrophobic domains with the material and their hydrophilic domains with the biological environment to create a substantial reduction in surface energy. This reduction outweighs the entropic cost of the conformational change, which also thermodynamically favors protein adsorption onto a hydrophobic material surface.[3] Among all the different parameters, water-mediated hydrophobic/hydrophilic and hydration forces were considered as the major factors in protein adsorption, a view that culminated in the concept of "Berg's law" or "Berg's limit".[4] This concept describes which surfaces can promote protein adsorption depending on their hydrophobic or hydrophilic properties. Surfaces are hydrophobic if their static water contact angle θ is bigger than a critical value of 65°. On hydrophilic surfaces with $\theta < 65°$, proteins are not able to displace water from the surface and therefore they do not adsorb onto them. Therefore, decreasing surface hydrophobicity is a widely used method to reduce interfacial energy and make the protein adsorption less favorable. Much effort has been made to regulate surface wetting properties, for example, hydrophilic polymer grafting, hydrogel network formation, layer-by-layer (LbL) assembly, and other chemical/physical surface modification technologies.[5] To dynamically control material surfaces/interface properties, some stimuli-responsive molecules have been introduced as "smart" coatings and the resulting interfacial properties could be tuned by external stimuli.[6] Among various options, light has attracted much attention as it can noninvasively regulate protein/cell–material surface interactions with high spatiotemporal precision.[7] Spiropyran (SP) is a well-known and well-investigated photochrome for its light-induced spiropyran-to-merocyanine (SP–MC) isomerization.[8] SP is usually nonpolar and hydrophobic in its closed form. Under UV light irradiation, SP dynamically isomerizes to the MC form (open form) and converts into a polar, hydrophilic, and zwitterion molecule.[9] Unlike other common photochromes, spiropyran itself has two different states (SP and MC), which could reversibly intercalate into the DNA helix,[10] regulate enzyme activity,[11] and even specifically interact with cell surface protein fibronectin.[12] Herein, we integrated light-responsive spiropyran groups into our mussel-inspired coating technology[13] to fabricate a light-regulated functional surface coating (Scheme 1). According to the empirical "Whitesides' design rules",[14] both the hydrated hydrophilic polymers and zwitterions distributing on the materials surface can great-

[a] L. Yu, C. Schlaich, Y. Hou, J. Zhang, Prof. R. Haag
Institute of Chemistry and Biochemistry
Freie Universität Berlin, Takustrasse 3, Berlin 14195 (Germany)
E-mail: haag@chemie.fu-berlin.de

[b] Dr. P.-L. M. Noeske
Fraunhofer Institute for Manufacturing Technology and
Advanced Materials IFAM, Wiener Strasse 12, 28359 Bremen (Germany)

Supporting information and the ORCID identification number(s) for the author(s) of this article can be found under:
https://doi.org/10.1002/chem.201801051. It contains methods and any associated references.

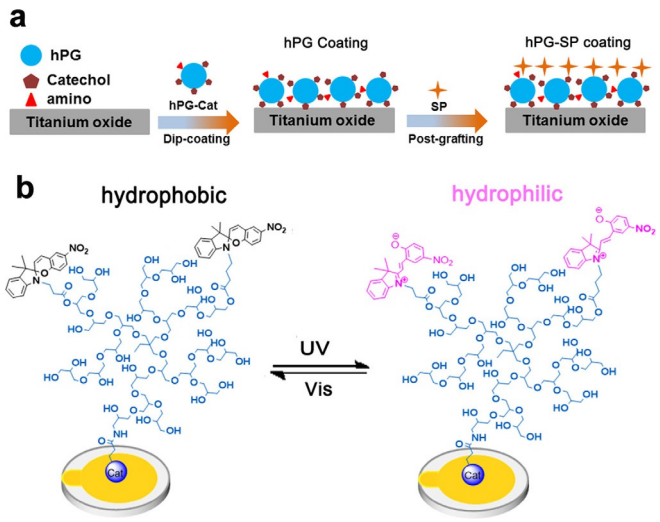

Scheme 1. (a) Preparation of hPG-SP coatings on titanium oxide (TiO_2) substrate. (b) The spiropyran moiety on hPG-SP coatings can be photochemically converted between the hydrophobic SP form and hydrophilic zwitterionic MC form.

ly reduce nonspecific protein adsorption. Therefore, the resulting functional coating exhibited an interesting noninvasive, light-controlled protein adsorption and cell adhesion behavior. Moreover, polyglycerol (PG) has a highly flexible aliphatic polyether backbone with multiple hydrophilic functional groups. This polar polymer has been proven to have high affinity with water molecules to generate a hydration layer[13b,c] that serves as an efficient barrier to nonspecific protein adsorption.[1b,15] In the hPG-SP coatings, the presented hPG provided a robust bioinert background to suppress the nonspecific protein adsorption and cell adhesion. Benefiting from this and the reversible isomerization between SP and MC, the detachment of the adsorbed proteins, cells, and even dense cell sheets was also realized on this functional coating surface.

Results and Discussion

Amino functional hyperbranched polyglycerols (hPG, 10% amino groups) were synthesized by the ring-opening anionic polymerization of glycidol, followed by O-methylation, azide substitution, and the Staudinger reaction according to a reported protocol.[13b] The anchoring catechol groups were then grafted onto amino functional hPGs by amide coupling, resulting in catecholic hPGs with 7.5% functional degree (hPG-Cat). The catechol groups, which are found in mussel adhesive proteins[16] and bacterial siderophores,[17] can adhere on virtually almost any material surface and has been proven to be a powerful anchor for surface modification.[18] Because of their highly branched architecture and multiple anchoring catechol groups, hPG-Cat can form stable coatings on many different substrates including metal, metal oxides, ceramic, and even polymeric material surfaces. Research has indicated that a charge-transfer complex could be formed between the catechol and TiO_2 surface,[19] resulting in the strongest bonding of catecholic macromolecules onto TiO_2. Therefore, to ensure the stability of the hPG coating, especially the stability during post-modification, TiO_2 was utilized as the model substrate in the following unless otherwise specified. A quartz crystal microbalance (QCM) with dissipation was employed to analyze the adsorption of the hPG-Cat polymer on the TiO_2 sensors. The results show that the hydrated mass of the adsorbed hPG-Cat on the sensor surfaces was about 1200 ng cm^{-2} (Figure S1 in the Supporting Information) for 5 h dynamic online coating in basic conditions (pH 8.5, MOPS buffer; 3-(*N*-morpholino)propanesulfonic acid). The stability of the coatings was tested by rinsing the adsorbed polymers with 2% w/w sodium dodecyl sulfate (SDS). There was no significant detachment of hPG-Cat from the TiO_2 surface owing to the stable multivalent catecholic anchoring. The dry thickness of the resulting polymer coating layer was about (12.9 ± 0.1) nm measured by ellipsometry. To guarantee all spiropyran groups distribute on the top layer of the coating surface, spiropyran was post-grafted onto the hPG coating through a surface ester reaction catalyzed by EDCI/DMAP (1-ethyl-3-(3-dimethylaminopropyl)carbodiimide/4-dimethylaminopyridine). X-ray photoelectron spectroscopy (XPS) analysis was employed to quantitatively determine the chemical composition of the coating. The atomic ratios of O/Ti, C/Ti, and N/Ti were significantly changed after hPG-Cat dip-coating and SP post grafting (Figure S2 in the Supporting Information). In the spectrum of N 1s, peaks corresponding to polydopamine[20] and imide species in hPG-Cat were observed at (396.0 ± 0.1) eV/(397.0 ± 0.1) eV (including the nitride species from titania during preparation in vacuum, which could also be found in the N 1s spectrum of bare TiO_2), and (399.8 ± 0.1) eV, respectively (Figure 1a). After SP grafting, two additional significant new intense peaks appeared at binding energies (BEs) of (401.9 ± 0.2) and (405.9 ± 0.1) eV, assigned to the am-

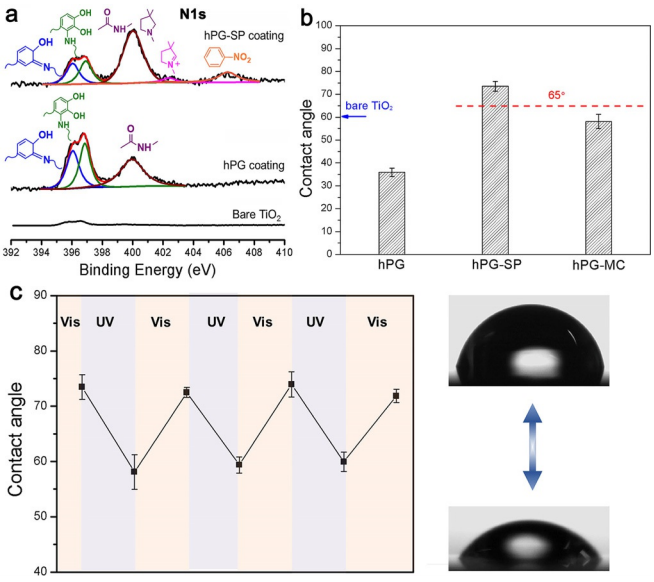

Figure 1. (a) The deconvoluted XPS N 1s signal curves of hPG-SP coatings, hPG coating, and the corresponding pristine TiO_2 substrate. (b) Average static water contact angle of the bare substrate surface, hPG coating, hPG-SP coating, and the hPG-MC coating. The red line indicates the "Berg's limit". (c) Wettability switching on a hPG-SP coating surface (5 min irradiation with λ = 365 nm UV light, 30 min irradiation with λ = 530 nm visible light).

monium nitrogen (MC in open form)[21] and the characterized nitro group of spiropyran.[22] The indoline nitrogen in spiropyran localized at (399.4 ± 0.1) eV and combined with the imide nitrogen.[23] The SP grafting density was roughly calculated as 1.2% (to all -OH groups in hPG backbone) based on the area ratio of the nitro group to amide group. The corresponding C 1s and O 1s spectra of the hPG coating and hPG-SP coating were also analyzed and are shown in Figure S3 in the Supporting Information. In the spectra of O 1s, the peak area ratio of (532.7 ± 0.1) eV (assigned to the ether group, carbonyl group, and ester group) and (531.5 ± 0.1) eV (assigned to the hydroxyl group in the PG backbone) was increased from 2.4 to 6.4 after SP grafting. This increase was ascribed to the formation of a new ester bond and the ester bond from grafted SP, indicating that the SP groups have been covalently bonded onto the hPG coating. Otherwise, the coating thickness slightly increased to (14.0 ± 0.4) nm after SP functionalization. Both of these findings strongly verified the success and effect of the surface modification.

The wetting property/behavior of the surface was also dramatically changed after hydrophilic hPG coating and hydrophobic SP grafting (Figure 1 b and Table S1 in the Supporting Information). Polyglycerol is composed of hydrophilic repeating units, which can hydrogen bond with water molecules and are hence highly hydrated in water.[15b] The static water contact angle of the hPG coating was only about 36° (Table S1 in the Supporting Information). However, the spiropyran in its closed ring form is typically hydrophobic. Therefore, the surface energy of the modified coating was greatly increased and resulted in a significantly greater water contact angle (73.5 ± 2.2)° after SP grafting (Figure 1 b). After exposing the hPG-SP coating to UV light (PLS-0365-010-11-C LED UV lamp, 365 nm; 42 mW cm^{-2}) for 5 min, accompanied with the isomerization from SP to MC, the surface hydrophilicity was gradually increased (Figure 1 b). The resulting static water contact angle was (58.1 ± 3.1)°, which is in the range of hydrophilic surfaces according to "Berg's law". The hydrophobicity of the hPG-SP coating can be reversibly switched back by 30 min of visible light irradiation (PLS-0530-010-15-C, 530 nm, 30 mW cm^{-2}). As shown in Figure 1 c, the contact angles can reversibly and reproducibly be switched from approximately 78° to 59°.

As mentioned above, the nonspecific protein adsorption on material surfaces is highly related to the surface wetting property. In this respect, a quartz crystal microbalance (QCM) with dissipation was employed to evaluate the nonspecific protein adsorption on the hPG-SP coating surface. Fibrinogen (Fib) was selected as the model protein because it is relevant to nonspecific adsorption and biofilm formation[14b] and is commonly used to evaluate the biocompatibility of artificial surfaces.[24] The amount of Fib adsorbed onto the testing surface was calculated from the frequency (Δf) shift of the QCM sensorgrams by applying the Kevin–Voigt model. The representative QCM sensorgrams of protein adsorption are shown in Figure S4 in the Supporting Information. As expected, the hPG coating exhibited a good antifouling performance as the highly hydrated polyglycerol chain served as an energetic barrier to nonspecific protein adsorption.[15b] However, after SP grafting, the protein adsorption was increased nearly 31-fold owing to the contribution of spiropyran to surface hydrophobicity (Table S1 in the Supporting Information). As aforementioned, the surface wetting property of the hPG-SP coating could be plainly tuned by UV light irradiation based on the photoisomerization of spiropyran groups. After irradiating with UV light for 10 min, the grafted hydrophobic SP gradually isomerized into hydrophilic MC and, as a consequence, the resulting amount of adsorbed Fib remarkably decreased with 73.5% (Figure 2 a, Figure S4 in the Supporting Information). The hydrophilic and zwitterionic MC groups, similar to phosphorylcholine[25] and betaine derivatives,[26] could strongly bind to water and create a hydration layer that resists the protein adsorption. On the hPG-SP coating surface, Fib protein patterns were successfully obtained by irradiating the coating surface with UV light through a designed patterned photomask prior to exposing the substrate to a protein suspension (30 mg mL^{-1}; Figure 2 b). A clearly contrasted protein pattern, in which Fib proteins were adsorbed mostly on the nonirradiated region, was obtained as expected. In the irradiated region, where the hydrophobic SP groups were isomerized into hydrophilic and zwitterionic MC groups, proteins did not or only weakly interact with the coating and then were washed away by rinsing with buffer. It is interesting that the surface water contact angle decreased from (73.5 ± 2.2)° to (58.1 ± 3.1)° after UV irradiation. The change of wetting property, together with the protein adsorption results, exactly coincided with the aforementioned concept of "Berg's law" or "Berg's limit". Although several drawbacks remain, this criterion has been extensively tested and utilized to explain many experimental results.[1b] The protein adsorption on hPG-SP coatings was effectively and efficiently controlled by light-induced hydrophobic/hydrophilic conversion. The conversion from ring-closed SP form to zwitterionic MC form is very quick and could

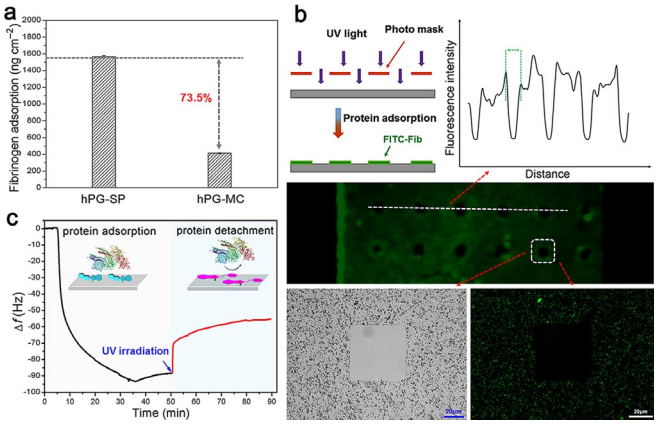

Figure 2. (a) Fibrinogen protein adsorption on hPG-SP and hPG-MC coating surfaces. (b) Fibrinogen protein adsorption on patterned hPG-SP coating surface. Top right: strategy for the preparation of a micropatterned surface. Top left: the corresponding relative intensities of FITC-Fib proteins distribution on the patterned surface. Bottom: the corresponding microscopic image and fluorescence microscopic image of FITC-Fib protein micropatterns. (c) QCM frequency (f) shift as a function of time during fibrinogen adsorption and its desorption after UV light irradiation.

rapidly reach an equilibrium within 5 min of irradiation (Figure S5 in the Supporting Information). Afterwards, the desorption of the adsorbed proteins was also performed and recorded by the QCM. The QCM chamber used here was specially equipped with a quartz window on the top (Figure S6 in the Supporting Information). Therefore, the UV light could pass through the quartz window and dynamically trigger the SP–MC isomerization in situ. As is well known, the spiro and mero isomers of the spiropyran moiety undergo dynamic balance and the photoisomerization quantum yield from the spiro to the mero form is only roughly 50% even in a polar environment.[27] Therefore, after 20 min of UV irradiation, approximately 52% (release% $= m_{released}/(m_{SP\,coating} - m_{MC\,coating})$) of the adsorbed Fib was released from the hPG-SP coating surface (Figure 2c), which was comparable to a previous report.[12a] In addition, this low release efficiency may also be related to the weak penetration of UV light through the strong reflection of water and Fib molecules.

Most adherent mammalian cells employ protein receptors on their membranes that can recognize and noncovalently bind with the extracellular matrix (ECM).[28] Therefore, light-modulated protein resistant surfaces are likely to be used to modulate cell adhesion. Moreover, molecular approaches to regulate cell–material interactions are desirable for cell biology and medical applications.[29] Among them, dynamically controlling cell adhesion on substrates is a fundamental issue because cell adhesion has profound effects on the cell fate and diverse cellular response behaviors.[30] Light-modulated cellular attachment on hPG-SP coating surfaces was performed by using NIH3T3 mouse fibroblast adhesion, which is involved in the tissue responses upon implantation into living tissue.[31] Initially, the spiropyran was mainly in the hydrophobic SP form, whereby the cells quickly adhered to the coating surface and began to spread during the first 1 h (Figure 3a), which could be concluded from the surface hydrophobicity and the unspecific interaction between SP and cell surface fibronectin.[12a,32] However, concerning the surface treated with UV irradiation (10 min), NIH3T3 cells were rarely observed on the hPG-MC surface and without significant spreading (Figure 3b), owing to the increased surface hydrophilicity and the weak interaction between MC and cell surface fibronectin.[33] The highly hydrated MC and PG chains formed a hydration layer to shield the interaction of cell membrane proteins with the substrate. As expected, almost no cells were found on the cell-resistant hPG coating (Figure S7 in the Supporting Information). The cell density on the surface of hPG, hPG-SP, and hPG-MC coatings was determined, and it is summarized in Figure 3c. This cell-resistant hPG-MC surface could also be switched back to a cell-attaching hPG-SP surface again with visible light irradiation ($\lambda = 550$ nm; Figure S8 in the Supporting Information). But at least 30 min of irradiation are required to convert most MC groups into SP groups.

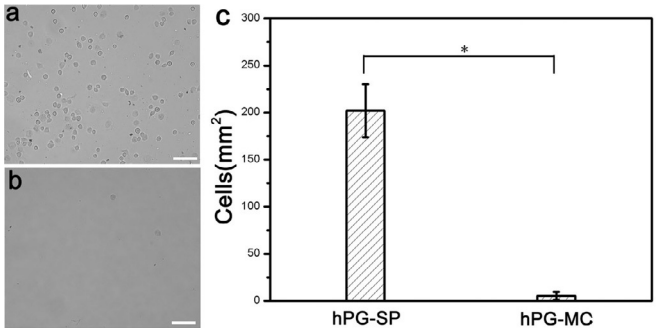

Figure 3. (a) NIH3T3 cell adhesion on the hPG-SP coating before and (b) after UV irradiation. Cells (4×10^4) were cultured with testing surfaces for 1 h. Images were collected after gentle PBS rinsing of the slides. Scale bar: 100 μm. (c) Number of NIH3T3 cells adhered on hPG-SP coating and hPG-MC coating (*$p < 0.0001$).

In addition, the light-regulated single cell and cell sheet detachment behavior was also investigated. Exposed to UV irradiation for 10 min, the spiropyran on the coating surface gave rise to hydrophilic/zwitterionic MC and the adhered spreading cells (Figure 4a) gradually shrunk and detached. After 1 h of incubation in the dark and subsequent gentle rinsing with phosphate buffered saline (PBS), almost no cells remained adhered to the hPG-MC coating surface (Figure 4b). We then examined whether this light-responsive coating could detach a dense cell sheet. After 10 min of UV irradiation and 1 h of incubation in the dark, the coating surface with a dense cell sheet was gently rinsed with PBS buffer. Compared with the original dense NIH3T3 cell sheet (Figure 4c), most of the adherent cells (>96%) detached from coating surface (Figure 4d). In contrast, there was no significant detachment from the control surface (Figure S9 in the Supporting Information). The nanoparticulate titanium dioxide (TiO_2) is highly photoactive and can generate reactive oxygen species (ROS) when exposed to ultraviolet radiation (UVR).[34] The released ROS may oxidize the polymer coating and/or is toxic to attached cells. The former effect has been excluded by the SP–MC–SP photoswitching cycle experiments. To test the potential toxicity of ROS and UV irradiation,

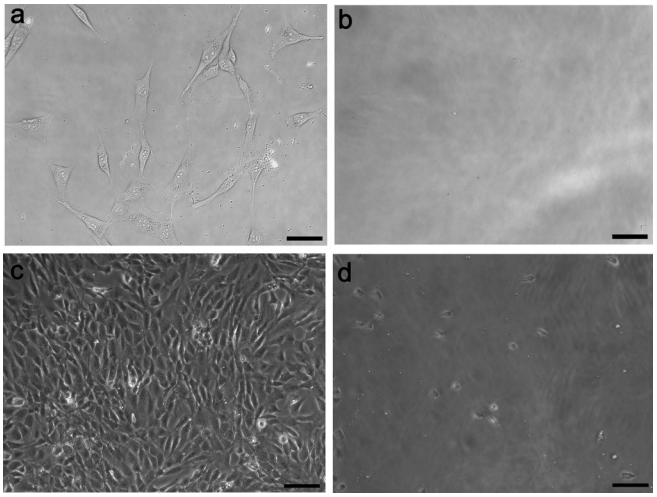

Figure 4. (a) The adhesion and (b) detachment of NIH3T3 single cell on the hPG-SP coating surface. Scale bar: 50 μm. (c) The NIH3T3 cell sheet on the hPG-SP coating surface. (d) NIH3T3 cell adhesion on the hPG-SP coating surface after 10 min UV irradiation, 1 h incubation at 37 °C in the dark, and finally gentle rinsing with PBS buffer. Scale bar: 50 μm.

live/dead staining verified that the cell viability did not significantly change after 10 min UV irradiation (Figure S10 in the Supporting Information). The result indicates that the photoactive of macro-planar TiO_2 surface under this timescale of UV irradiation is very low. This SP-functionalized coating could be used as an effective noninvasive cell adhesion/detachment platform for further biological investigations.

Conclusion

We have designed and developed an SP-based, light-responsive functional coating with a good bioinert PG background. In the normal state, the spiropyran groups on the coating surface were in the hydrophobic ring-closed SP form, which could promote the nonspecific protein adsorption and cell adhesion. After UV light irradiation, the spiro ring of SP opened and converted into a hydrophilic and zwitterionic MC. Both hydrophilicity and zwitterions contributed to the hydrated layer forming and therefore resisted the protein adsorption and cell adhesion. Moreover, the controllable adsorption/desorption of proteins and attachment/detachment of cells and even the dense cell sheet were also achieved on the SP-functionalized coating in a noninvasive mode. This functional coating exhibited a good perspective and potential utilization in bioresponsive surface modification and tissue engineering. The current system may be most appropriate for applications that facilitate sufficient UV illumination and may show limitations when substantial tissue penetration with light is required.

Experimental Section

Materials

All chemicals and solvents are reagent or HPLC grade, used as received, and purchased from Sigma (Steinheim, Germany) unless stated otherwise. Dialysis was performed in benzoylated cellulose tubes from Sigma–Aldrich (D7884, width: 32 mm, molecular weight cut-off (MWCO) 2000 g mol^{-1}). The deionized water used was purified by using a Millipore water purification system with a minimum resistivity of 18.0 MΩ cm$^{M->1}$. 3′,3′-Dimethyl-6-nitrol-spiro[2*H*-1-benzopyran-2,2′-indoline]-1′-ethanol (spiropyran, SP-OH, >93.0%) was purchased from TCI Europe. The hyperbranched polyglycerol (hPG), with $M_n \approx 5000$ g mol^{-1} and $M_w \approx 7500$ g mol^{-1}, was polymerized by a one-step ring-opening anionic polymerization (ROAP), as described in the literature.[35] Trimethylolpropane (TMP) was used as the initiator. Amino functional hyperbranched polyglycerols (hPG, 10% amino groups) were prepared according to a reported protocol.[13b]

Catecholic polyglycerol (hPG-Cat)

The polyglycerolamine (with 10% amino groups) and EDCI (3 equiv to amino groups) were dissolved in pH 4.8 MES (2-(*N*-morpholino)ethanesulfonic acid) aqueous buffer/methanol (1:1, v/v) mixed solvent. Then, 3,4-dihydroxyhydrocinnamic acid (3 equiv to amino groups) was added into the mixture and gently stirred overnight at room temperature. The product was purified by dialysis in methanol. The purified catecholic hPGs were dried under high vacuum and then stored under an argon atmosphere in the freezer. The corresponding grafting density of the catechol group on polymer chain was calculated based on the ^{1}H- NMR spectra. ^{1}H NMR (400 MHz; MeOD): $\delta = 6.80$–6.54 (Ar-H, 3H from catechol group), 4.00–3.40 (PG backbone), 2.76 (2H, COC**H**$_2$CH$_2$C), 2.47 (2H, COCH$_2$C**H**$_2$C), 1.41–1.39 (2H, CC**H**$_2$CH$_3$ of starter), 0.90 ppm (3H, CCH$_2$C**H**$_3$, of starter). The ^{1}H NMR spectrum is shown in Figure S11 in the Supporting Information.

3′,3′-Dimethyl-6-nitrol-spiro[2*H*-1-benzopyran-2,2′-indoline]-1′-succinate monoester (SP-COOH)

The carboxylic spiropyran was prepared according to reported protocols[36] with some modifications. SP-OH (1.6 g, 4.5 mmol) was added into anhydrous dichloromethane solution (120 mL) that contained succinic anhydride (2.7 g, 27 mmol), 4-dimethylaminopyridine (DMAP, 200 mg), and triethylamine (3 mL). The mixture was stirred at 40 °C for 24 h and then was washed three times sequentially with very diluted hydrochloric acid, saturated sodium bicarbonate solution, and deionized water. After condensing by rotary evaporation, the residue was purified by chromatography on silica gel eluted with ethyl acetate/chloroform (v/v, 1:6). The eluent was evaporated and gave a purple solid. ^{1}H NMR (400 MHz, $CDCl_3$): $\delta =$ 8.00 (m, 2H), 7.20 (td, $J = 7.18$ Hz, 1H), 7.09 (dd, $J = 7.08$, 7.06 Hz, 1H), 6.95–6.83 (m, 2H), 6.70 (dd, $J = 6.73$, 6.65 Hz, 2H), 5.88 (d, $J =$ 5.86 Hz, 1H), 4.37–4.08 (m, 2H), 3.57–3.32 (m, 2H), 2.54 (m, 4H), 1.27 (s, 3H), 1.15 ppm (s, 3H). The ^{1}H NMR spectrum is shown in Figure S12 in the Supporting Information.

Dip-coating of hPG-Cat

TiO_2 slides were first cleaned ultrasonically in water and methanol, and then treated with UV/ozone (UV/Ozone ProCleaner, Bioforce Nanosciences) for 20 min before use. All the QCM chips were cleaned according to the standard cleaning protocol from LOT (LOT-Quantum Design GmbH, Darmstadt, Germany). To prepare hPG-Cat coatings, the cleaned TiO_2 slides were immersed into the solution of 1 mM hPG-Cat at pH 8.5 in 3-(*N*-morpholino)propanesulfonic acid buffer (MOPS; 0.1 M) at room temperature for 12 h. After that, the slides were thoroughly rinsed with water and then dried by using a N_2 stream.

Post-surface modification with spiropyran

To guarantee all responsive groups distributed on the upper layer of the coating, spiropyran was post grafted onto the hPG-Cat coating by ester reaction. SP-COOH (1 equiv), EDCI (1.2 equiv), and DMAP (0.2 equiv) wee dissolved in absolute DMF under argon atmosphere. hPG-Cat coated slides were then immersed into the prepared 50 mM SP-COOH solution. After 24 h reaction at room temperature with gentle shaking, the slide was thoroughly rinsed with DMF and water, and then dried by using a N_2 stream.

Water contact angle

Static contact angle measurements were performed by using a contact angle goniometer (DataPhysics Instruments, Germany) with the sessile drop method. A liquid drop of 2 μL Milli-Q water was placed on the substrate and allowed to equilibrate for 15 s at room temperature. At least fifteen measurements from five parallel coating samples were averaged to get a reliable value. Error bars indicate standard deviation (SD).

X-ray photoelectron spectroscopy (XPS)

The XPS spectra for coating surfaces were taken by using a Kratos system with the following acquisition parameters: base pressure 4×10^{-10} mbar; sample neutralization by applying low energy electrons (up to 5 eV); hybrid mode (electrostatic and magnetic lenses are used) for acquiring detailed spectra, and electrostatic mode for obtaining substrate signal intensities for evaluating adsorbate layer thickness; take off angle of electrons, 0°; pass energy, 20 eV in high-resolution spectra and 160 eV in survey spectra; and excitation of photoelectrons by monochromatic $Al_{K\alpha}$ radiation ($h\nu=$ 1486.6 eV), which was used at 300 W (15 kV×20 mA). The analysis area was elliptically shaped with main axes of 300 μm×700 μm.

Quartz crystal microbalance (QCM) with dissipation

A quartz crystal microbalance (QCM, Q-Sense E1, Sweden) with dissipation was used to test the adsorption on the surfaces. QCM allows the monitoring of changes in resonance frequency (Δf) and dissipation (ΔD) of a piezoelectric quartz crystal as a function of time. f and D were recorded at the fundamental frequency (4.95 MHz) and its third, fifth, seventh, ninth, eleventh, and thirteenth overtones. Only the third overtone is shown in the sensorgrams. To measure the protein adsorbed onto the functional surface, coated sensors were inserted into the flow chamber and incubated in pH 7.4 in 4-(2-hydroxyethyl)-1-piperazine ethanesulfonic acid (HEPES, 0.1 mol L^{-1}, pH 7.4, and 150 mmol L^{-1} NaCl) buffer. After baseline equilibration, the protein solution (1 mg mL^{-1}, Fib, 340 kDa) was pumped into the flow chamber. After 30 min, the surface was rinsed with HEPES buffer again for another 15 min. The flow rate used for all experiments was 0.1 mL min^{-1}, and the temperature was 25 °C. The Sauerbrey equation was used to calculate the mass of the adsorbates ($\Delta m=C\times\Delta f$, where Δm is the change in mass, C is the mass sensitivity constant of the quartz crystal (-17.7 ng cm^{-2} Hz^{-1}), and Δf is the overtone-normalized frequency change.

Cell adhesion

Cell adhesion experiments on coated slides were done with adherent NIH3T3 murine fibroblast cells (ACC no. 59, DSMZ, Braunschweig, Germany). Cells were collected from Petri dishes by incubation in trypsin (dilution 1:250) for 5 min at 37 °C. The trypsin was removed from the cell suspension by centrifugation; the top layer was removed, and the remaining cells were re-suspended in fresh medium. The coated slides were incubated with 4×10^4 cells in 1 mL of cell medium (cell number was determined with a Neubauer chamber) at 37 °C and 5% CO_2. At a set time, the coated slides were taken out and gently rinsed with PBS buffer. The adhering cells were observed directly with a microscope (TELAVAL 31, Zeiss, Germany). The coated slides adhered with single cells and dense cell sheets were prepared by a similar protocol. hPG-SP coated slides were incubated with 1×10^4 cells in 1 mL of NIH3T3 cell medium (cell number was determined with a Neubauer chamber) at 37 °C and 5% CO_2. After 3 h, the slides with spread and separated cells were taken out and gently rinsed with PBS buffer for further detachment experiments. The coated slides with dense cell sheets were incubated over 2 days and then gently rinsed with PBS buffer.

Acknowledgments

This work was supported by the Chinese Scholar Council (CSC) and the SFB 658 of the German Science Foundation and Helmholtz Virtual Institute on "Multifunctional Biomaterials for Medicine". We thank Dr. Qiang Wei for helpful discussions on the protein adsorption pattern on the hPG-SP coating surface. We thank Dr. Pamela Winchester for language polishing.

Conflict of interest

The authors declare no conflict of interest.

Keywords: antifouling · controlling cell adhesion · functional coatings · photochemistry · spiropyranes

[1] a) C. Blaszykowski, S. Sheikh, M. Thompson, *Chem. Soc. Rev.* **2012**, *41*, 5599 – 5612; b) Q. Wei, T. Becherer, S. Angioletti-Uberti, J. Dzubiella, C. Wischke, A. T. Neffe, A. Lendlein, M. Ballauff, R. Haag, *Angew. Chem. Int. Ed.* **2014**, *53*, 8004 – 8031; *Angew. Chem.* **2014**, *126*, 8138 – 8169; c) I. Banerjee, R. C. Pangule, R. S. Kane, *Adv. Mater.* **2011**, *23*, 690 – 718; d) S. Jiang, Z. Cao, *Adv. Mater.* **2010**, *22*, 920 – 932.

[2] K. Nakanishi, T. Sakiyama, K. Imamura, *J. Biosci. Bioeng.* **2001**, *91*, 233 – 244.

[3] P. Gong, D. W. Grainger, *Microarrays: Vol. 1 of Synthesis Methods*, Humana, New York, **2007**, pp. 59 – 92.

[4] E. A. Vogler, *Adv. Colloid Interface Sci.* **1998**, *74*, 69 – 117.

[5] Q. Wei, R. Haag, *Mater. Horiz.* **2015**, *2*, 567 – 577.

[6] a) H. Nandivada, A. M. Ross, J. Lahann, *Prog. Polym. Sci.* **2010**, *35*, 141 – 154; b) T. Chen, R. Ferris, J. Zhang, R. Ducker, S. Zauscher, *Prog. Polym. Sci.* **2010**, *35*, 94 – 112; c) O. Nachtigall, C. Kördel, L. H. Urner, R. Haag, *Angew. Chem. Int. Ed.* **2014**, *53*, 9669 – 9673; *Angew. Chem.* **2014**, *126*, 9824 – 9828.

[7] J.-F. Gohy, Y. Zhao, *Chem. Soc. Rev.* **2013**, *42*, 7117 – 7129.

[8] a) G. Berkovic, V. Krongauz, V. Weiss, *Chem. Rev.* **2000**, *100*, 1741 – 1754; b) S. Kumar, J. T. van Herpt, R. Y. Gengler, B. L. Feringa, P. Rudolf, R. C. Chiechi, *J. Am. Chem. Soc.* **2016**, *138*, 12519 – 12526.

[9] a) M. Dübner, N. D. Spencer, C. Padeste, *Langmuir* **2014**, *30*, 14971 – 14981; b) D. Kessler, F. D. Jochum, J. Choi, K. Char, P. Theato, *ACS Appl. Mater. Interfaces* **2011**, *3*, 124 – 128.

[10] J. Andersson, S. Li, P. Lincoln, J. Andréasson, *J. Am. Chem. Soc.* **2008**, *130*, 11836 – 11837.

[11] Y. Song, C. Xu, W. Wei, J. Ren, X. Qu, *Chem. Commun.* **2011**, *47*, 9083 – 9085.

[12] a) A. Higuchi, A. Hamamura, Y. Shindo, H. Kitamura, B. O. Yoon, T. Mori, T. Uyama, A. Umezawa, *Biomacromolecules* **2004**, *5*, 1770 – 1774; b) J.-i. Edahiro, K. Sumaru, Y. Tada, K. Ohi, T. Takagi, M. Kameda, T. Shinbo, T. Kanamori, Y. Yoshimi, *Biomacromolecules* **2005**, *6*, 970 – 974; c) D. He, Y. Arisaka, K. Masuda, M. Yamamoto, N. Takeda, *Acta Biomater.* **2017**, *51*, 101 – 111.

[13] a) Q. Wei, K. Achazi, H. Liebe, A. Schulz, P. L. M. Noeske, I. Grunwald, R. Haag, *Angew. Chem. Int. Ed.* **2014**, *53*, 11650 – 11655; *Angew. Chem.* **2014**, *126*, 11834 – 11840; b) Q. Wei, T. Becherer, P. L. M. Noeske, I. Grunwald, R. Haag, *Adv. Mater.* **2014**, *26*, 2688 – 2693; c) L. Yu, C. Cheng, Q. Ran, C. Schlaich, P.-L. M. Noeske, W. Li, Q. Wei, R. Haag, *ACS Appl. Mater. Interfaces* **2017**, *9*, 6624 – 6633.

[14] a) R. G. Chapman, E. Ostuni, S. Takayama, R. E. Holmlin, L. Yan, G. M. Whitesides, *J. Am. Chem. Soc.* **2000**, *122*, 8303 – 8304; b) E. Ostuni, R. G. Chapman, R. E. Holmlin, S. Takayama, G. M. Whitesides, *Langmuir* **2001**, *17*, 5605 – 5620.

[15] a) M. Weinhart, I. Grunwald, M. Wyszogrodzka, L. Gaetjen, A. Hartwig, R. Haag, *Chem. Asian J.* **2010**, *5*, 1992 – 2000; b) C. Siegers, M. Biesalski, R. Haag, *Chem. Eur. J.* **2004**, *10*, 2831 – 2838; c) G. Gunkel, M. Weinhart, T. Becherer, R. Haag, W. T. Huck, *Biomacromolecules* **2011**, *12*, 4169 – 4172; d) E. Moore, B. Delalat, R. Vasani, G. McPhee, H. Thissen, N. H. Voelcker, *ACS Appl. Mater. Interfaces* **2014**, *6*, 15243 – 15252; e) L. Yu, Y. Hou, C.

Cheng, C. Schlaich, P.-L. M. Noeske, Q. Wei, R. Haag, *ACS Appl. Mater. Interfaces* **2017**, *9*, 44281 – 44292.
[16] a) J. H. Waite, M. L. Tanzer, *Science* **1981**, *212*, 1038 – 1040; b) J. H. Waite, X. Qin, *Biochemistry* **2001**, *40*, 2887 – 2893.
[17] K. N. Raymond, E. A. Dertz, S. S. Kim, *Proc. Natl. Acad. Sci. USA* **2003**, *100*, 3584 – 3588.
[18] a) H. Lee, S. M. Dellatore, W. M. Miller, P. B. Messersmith, *Science* **2007**, *318*, 426 – 430; b) G. P. Maier, M. V. Rapp, J. H. Waite, J. N. Israelachvili, A. Butler, *Science* **2015**, *349*, 628 – 632; c) S. Zürcher, D. Wäckerlin, Y. Bethuel, B. Malisova, M. Textor, S. Tosatti, K. Gademann, *J. Am. Chem. Soc.* **2006**, *128*, 1064 – 1065.
[19] R. Rodríguez, M. A. Blesa, A. E. Regazzoni, *J. Colloid Interface Sci.* **1996**, *177*, 122 – 131.
[20] Y.-P. Zhu, Y.-P. Liu, Z.-Y. Yuan, *Chem. Commun.* **2016**, *52*, 2118 – 2121.
[21] J. Allouche, A. Le Beulze, J.-C. Dupin, J.-B. Ledeuil, S. Blanc, D. Gonbeau, *J. Mater. Chem.* **2010**, *20*, 9370 – 9378.
[22] O. Ivashenko, J. T. van Herpt, B. L. Feringa, P. Rudolf, W. R. Browne, *J. Phys. Chem. C* **2013**, *117*, 18567 – 18577.
[23] O. Ivashenko, J. T. van Herpt, B. L. Feringa, P. Rudolf, W. R. Browne, *Langmuir* **2013**, *29*, 4290 – 4297.
[24] E. Ostuni, R. G. Chapman, M. N. Liang, G. Meluleni, G. Pier, D. E. Ingber, G. M. Whitesides, *Langmuir* **2001**, *17*, 6336 – 6343.
[25] V. A. Tegoulia, W. Rao, A. T. Kalambur, J. F. Rabolt, S. L. Cooper, *Langmuir* **2001**, *17*, 4396 – 4404.
[26] Z. Zhang, H. Vaisocherova, G. Cheng, W. Yang, H. Xue, S. Jiang, *Biomacromolecules* **2008**, *9*, 2686 – 2692.
[27] a) M.-Q. Zhu, L. Zhu, J. J. Han, W. Wu, J. K. Hurst, A. D. Li, *J. Am. Chem. Soc.* **2006**, *128*, 4303 – 4309; b) L.-X. Yu, Y. Liu, S.-C. Chen, Y. Guan, Y.-Z. Wang, *Chin. Chem. Lett.* **2014**, *25*, 389 – 396.
[28] R. O. Hynes, *Cell* **1987**, *48*, 549 – 554.
[29] a) M. Mrksich, *Chem. Soc. Rev.* **2000**, *29*, 267 – 273; b) M. Wiemann, R. Niebuhr, A. Juan, E. Cavatorta, B. J. Ravoo, P. Jonkheijm, *Chem. Eur. J.* **2018**, *24*, 813 – 817.
[30] B. M. Gumbiner, *Cell* **1996**, *84*, 345 – 357.
[31] B. D. Ratner, *J. Dental Educ.* **2001**, *65*, 1340 – 1347.
[32] N. Wang, Y. Li, Y. Zhang, Y. Liao, W. Liu, *Langmuir* **2014**, *30*, 11823 – 11832.
[33] a) W. Li, Z. Chen, L. Zhou, Z. Li, J. Ren, X. Qu, *J. Am. Chem. Soc.* **2015**, *137*, 8199 – 8205; b) Z. Chen, L. Zhou, W. Bing, Z. Zhang, Z. Li, J. Ren, X. Qu, *J. Am. Chem. Soc.* **2014**, *136*, 7498 – 7504.
[34] R. J. Miller, S. Bennett, A. A. Keller, S. Pease, H. S. Lenihan, *PLoS One* **2012**, *7*, e30321.
[35] a) A. Sunder, R. Mülhaupt, R. Haag, H. Frey, *Adv. Mater.* **2000**, *12*, 235 – 239; b) A. Sunder, R. Hanselmann, H. Frey, R. Mülhaupt, *Macromolecules* **1999**, *32*, 4240 – 4246.
[36] a) L. Chen, W. Wang, B. Su, Y. Wen, C. Li, Y. Zhou, M. Li, X. Shi, H. Du, Y. Song, *ACS Nano* **2014**, *8*, 744 – 751; b) L. Ming, Z. K. Si, Q. Zhang, Q. R. Sheng, M. Z. Xue, Y. G. Liu, *Res. Chem. Intermed.* **2015**, *41*, 3017 – 3029.

Manuscript received: March 1, 2018
Accepted manuscript online: March 26, 2018
Version of record online: May 2, 2018